



# Isolation of high purity guard cell protoplasts of *Arabidopsis thaliana* for omics research

Chenchen Zhao<sup>1</sup> · David Randall<sup>1</sup> · Paul Holford<sup>1</sup> · Anthony M. Haigh<sup>1</sup> · Zhong-Hua Chen<sup>1,2</sup>

Received: 23 March 2019 / Accepted: 1 July 2019 / Published online: 6 July 2019  
© Springer Nature B.V. 2019

## Abstract

Stomata are unique plant structures responsible for photosynthesis, transpiration and innate immunity to pathogens, and guard cells are one of the most studied cell types with respect to plant cell functioning, signalling, and stress responses. The ability to easily purify large quantities of high purity guard cell protoplasts (GCPs) would facilitate further studies, as current methods for GCP isolation are barely sufficient for omics research. Here, we report a new procedure for isolating high purity GCPs. For the isolation of GCPs, detached epidermal peels were used to extract GCPs instead of whole leaves. GCPs and mesophyll cell protoplasts (MCPs) were found to have diameters of 2.5–9.1  $\mu\text{m}$  and 6.5–43.5  $\mu\text{m}$ , respectively. The overlap in sizes of GCPs and MCPs suggests that blending and filtering of whole leaves used in previous methods may not necessarily avoid contamination with MCPs during GCP extraction. There were, on average,  $8.4 \pm 0.18$  chloroplasts in GCPs and  $34.6 \pm 1.5$  in MCPs. For MCPs and GCPs with similar sizes, there were fourfold more chloroplasts in MCPs, which made MCPs readily distinguishable from GCPs by microscopic inspection. The protocol enabled the isolation of over  $1.44 \times 10^6$  GCPs from about 150  $\text{cm}^2$  *Arabidopsis* abaxial epidermis with over 97% purity. These protocols provide an advance in isolating sufficient, high purity, and viable protoplasts for RNA extraction and transcriptomic analysis. The application of this protocol to other plant species may accelerate the research and development of plant cell-type specific omics.

**Keywords** Epidermal peels · Protoplast isolation · Transcriptomics · Chloroplasts · Mesophyll cell protoplasts

## Introduction

Stomatal guard cells regulate gaseous fluxes, plant water status and photosynthesis by closing or opening stomata, which makes this unique cell type significant to terrestrial ecosystems and agriculture (Misra et al. 2015; Zhao et al. 2018). Stomatal guard cells are a key plant evolutionary innovation, facilitating specialized signalling networks that have enabled plants to colonise land and adapt to terrestrial environments (Cai et al. 2017; Chen et al. 2017; Zhao et al. 2019). In addition, stomata also have significant roles associated with plant tolerance to abiotic stresses such as drought, salinity, high light, and cold (Zhu 2016; Hedrich and Shabala 2018; Chen et al. 2019). Drought stress-induced

stomatal closure involves the regulation of abscisic acid (ABA) signalling, secondary messengers such as reactive oxygen species (ROS) and nitric oxide (NO), and ion channels and transporters in guard cells (Ward and Schroeder 1994; Guo 2002; Vahisalu et al. 2008; Chen et al. 2016, 2019; Lind et al. 2015; Zhao et al. 2018). For instance, over-expressing *Epidermal Patterning Factors* (EPFs) reduces stomatal density resulting in improved drought tolerance and improved instantaneous and long-term water use efficiency without altering plant photosynthetic capacity in *Arabidopsis* (Franks et al. 2015) and barley (Hughes et al. 2017). Many pathogens access the internal tissues of plants through open stomata, so plants have evolved mechanisms to induce stomatal closure as an important innate immune response, involving complex signalling pathways that regulate stomatal closure (Melotto et al. 2006; Gudesblat et al. 2009; Zeng et al. 2010).

Rapid progress in single cell-based studies in mammals, especially in humans, has enabled researchers to focus on cell-specific diseases, responses and functions (Quintana et al. 2008; Brennecke et al. 2013; Petropoulos et al. 2016).

✉ Zhong-Hua Chen  
z.chen@westernsydney.edu.au

<sup>1</sup> School of Science and Health, Western Sydney University, Penrith, NSW 2751, Australia

<sup>2</sup> Hawkesbury Institute for the Environment, Western Sydney University, Penrith, NSW 2751, Australia

In plants, guard cells are important models for studying cell-specific traits and functions due to their measurable molecular, cellular and physiological responses to abiotic and biotic stresses (Mäser et al. 2003; Chen et al. 2012), resulting in the development of guard cell-specific research tools that are especially useful for omics (Yang et al. 2008; Robaina-Estévez et al. 2017). The integration of omics from multiple approaches represents a key aspect towards a high level of understanding of biological activities in a specific plant cell-type. For instance, combining epigenomic and transcriptomic data sets can reveal the influence of cell-specific DNA modifications on gene activity. The integration of transcriptomes, proteomes, and metabolomes of single cell types provides better access to the relationship of RNAs and their downstream products (Wu et al. 2013; Hetzel et al. 2016; Wang et al. 2016; Libault et al. 2017). However, the applications of these technologies in plant cells are limited due to the accessibility of large quantities of high purity protoplasts, and potential contamination with other cell types during isolation procedures.

The isolation of guard cell protoplasts (GCPs) was pioneered using *Allium cepa* and *Nicotiana tabacum* (Zeiger and Hepler 1976). Protocols for extracting GCPs from *Vicia faba* were also developed to study the starch content of GCPs (Schnabl et al. 1978; Kruse et al. 1989). Later, GCP isolation protocols were developed for numerous species such as *Paphiopedilum harrisianum* (Zeiger 1981), *Commelina communis* (Fitzsimons and Weyers 1983), *Zea mays* (Fairley-Grenot and Assmann 1992), *Beta vulgaris* (Hall et al. 1996), *Arabidopsis thaliana* (Pandey et al. 2002), and *Solanum lycopersicum* (Yao et al. 2018). Apart from enzyme digestion-based protoplast isolation, methodologies such as laser-capture microdissection have been developed for ion channel activities of single guard cells using patch clamp techniques (Henriksen and Assmann 1997) and were later used for studying guard cell transcriptome profiling (Aubry et al. 2016).

Guard cells are derived from meristemoids that also give rise to leaf epidermal cells (Palevitz 1981; Zhao and Sack 1999). Therefore, it is difficult to physically isolate intact guard cells without damaging their cell walls and associated components. In many cases, researchers have studied guard cell biology using guard cells in epidermal peels of *Vicia faba* (Chen et al. 2010; Wang and Blatt 2011) and *Arabidopsis* (Chen et al. 2012; Wang et al. 2012, 2013; Jezek and Blatt 2017) or using isolated guard cell protoplasts (Allen and Sanders 1994; Allen et al. 1999). However, current techniques for isolating and purifying large quantities of guard cell protoplasts need to be improved. Compared to mesophyll cell protoplasts (MCPs), GCPs are more fragile and sensitive to light and other stresses (Lahav et al. 2004). The long duration of the enzyme digestion processes used during extraction

decreases GCP yields and may lead to RNA degradation (Obulareddy et al. 2013). In *Arabidopsis*, blending 50 to 80 leaves and a two-step enzyme digestion have shortened the process to 2–3 h (Pandey et al. 2002). Although this method can reduce RNA decay, the high speed blending may induce stress-related genes (Hara et al. 2000; Raymond et al. 2000; Chung et al. 2008). In contrast, leaf epidermal peels can preserve guard cell activities up to 5 h, enabling many dynamic stomatal assays on epidermal peels (Hedrich et al. 1990; Chen et al. 2010, 2016; Meyer et al. 2010; Jin et al. 2013; Yang et al. 2017). Therefore, minimising mechanical damage with a gentle extraction procedure starting from epidermal peels may better preserve GCP integrity for studying their cellular signalling networks and omics. Here, we developed a practical method for extracting and purifying *Arabidopsis* GCPs from abaxial epidermal peels to avoid the destructive blending process. We also present optimised enzyme digestion times, temperatures, and other procedures. The method provides high purity *Arabidopsis* GCPs for high quality RNA sequencing experiments (Fig. 1).

## Results

### Chloroplast numbers distinguish GCPs from MCPs in *Arabidopsis thaliana*

The diameters of GCPs and MCPs ranged from 2.5 to 9.1  $\mu\text{m}$  and from 6.5 to 43.5  $\mu\text{m}$ , respectively (Fig. 2a, b). However, 70.9% of GCPs were within the range 5.8–9.1  $\mu\text{m}$  (Fig. 2b). The MCPs were, in general, larger than GCPs, with the majority of MCPs being between 15  $\mu\text{m}$  and 35  $\mu\text{m}$  in diameter (Fig. 2b). Thus, the data indicated that there is a size overlap between GCPs and MCPs.

The numbers of chloroplasts per protoplast were counted based on images in a single plane of view (Fig. 1a). The GCPs contained a small number of chloroplasts ( $8.4 \pm 0.18$  per protoplast) (Fig. 3b, c), and there was a significant correlation between GCP diameter and chloroplast numbers ( $y = 0.43x + 5.67$ ,  $R^2 = 0.32$ ,  $P < 0.01$ ) (Fig. 3a). In contrast, MCPs contained a greater number of chloroplasts at  $34.6 \pm 1.5$  per protoplast (Fig. 3b), and again there was a highly significant, linear correlation ( $y = 1.69x + 2.71$ ,  $R^2 = 0.91$ ,  $P < 0.01$ ) between MCP diameters and chloroplast numbers (Fig. 3a). There was no overlap in numbers of chloroplasts between GCPs and MCPs. For MCPs and GCPs with overlapping sizes (6.6–9.1  $\mu\text{m}$ ) (Fig. 3a), the protoplast sizes showed no statistical difference ( $P = 0.07$ ) but chloroplast numbers of MCPs were significantly higher than that of GCPs ( $P = 2.07 \times 10^{-17}$ ) (Fig. 3c).

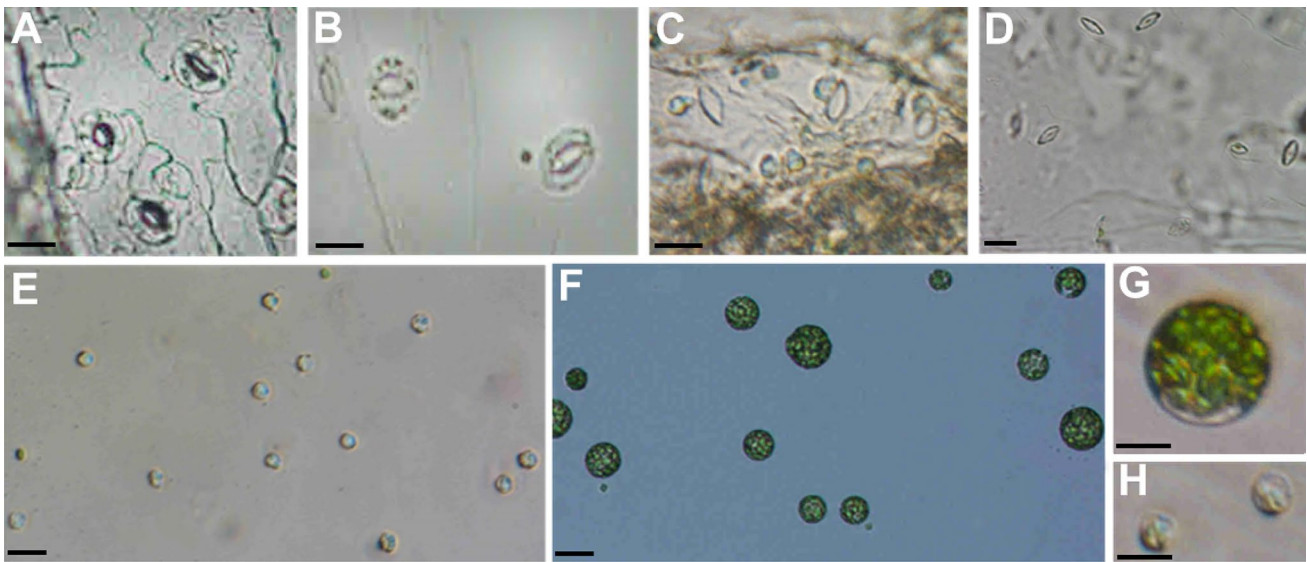


**Fig. 1** Representative images taken during isolation of guard cell protoplasts (GCPs) and mesophyll cell protoplasts (MCPs) of *Arabidopsis thaliana*. **a** Detached peel immersed in OB buffer showing epidermal cell walls and intact guard cells. **b** Peel after digestion with ESI. The peel has become more transparent but has intact guard cells and well digested epidermal cells. **c** Releasing GCPs during incubation with ESII for 40 min during which time **d** most of the guard cell pro-

toplasts have become detaching from stomata leaving only stomatal residues. **e** Round and healthy GCPs floating in Basic Solution and **f** round and green MCPs floating in Maintaining Solution. **g** A representative, normal, deep-green, MCP and **h** small, pale-green GCP. Scale bars in **a** to **f** represent 20  $\mu\text{m}$  while in **g** and **h**, scale bars represent 10  $\mu\text{m}$

### Protoplast purity, and RNA yield and quality in GCPs and MCPs

The purity of the extracted protoplasts was assessed based on their size and colour. Extracts of GCPs had a purity of 97.4% (Fig. 4a); the contaminating cells were less than 20  $\mu\text{m}$  in size and were dark green. The MCPs had a higher purity of 98.5% (Fig. 4a); the contaminating cells were less than 20  $\mu\text{m}$  in diameter and were pale green. Based on microscopic observation and calculation, approximately  $1.44 \times 10^6$  GCPs were extracted from 150  $\text{cm}^2$  of *Arabidopsis* leaf (Fig. 4b) and about  $7 \times 10^6$  MCPs from ten *Arabidopsis* leaves (Fig. 4b). Using these protoplasts for RNA extraction, GCPs yielded  $1.5 \pm 0.16$   $\mu\text{g}$  of total RNA from about 150  $\text{cm}^2$  of abaxial peels and MCPs produced  $2.5 \pm 0.66$   $\mu\text{g}$  from about 10 leaves (Fig. 4c).

RNA quality assessment showed clear 18S and 28S bands in the gel and high RNA integrity number (RIN) (Fig. 4d, e). All of the RNA sequencing runs yielded reliable quality sequence data with > 85% clean reads averaged at 16.43 million from GCPs and > 80% clean reads averaged at 19.2 million from MCPs, respectively (Table 1). RNA sequencing data from GCPs and MCPs both yielded large numbers of raw and clean reads and low numbers (less than 5%, mean) of unmapped reads (Table 2). For both GCPs and MCPs, 95% of total reads were successfully mapped to the *Arabidopsis* genome (Table 2).

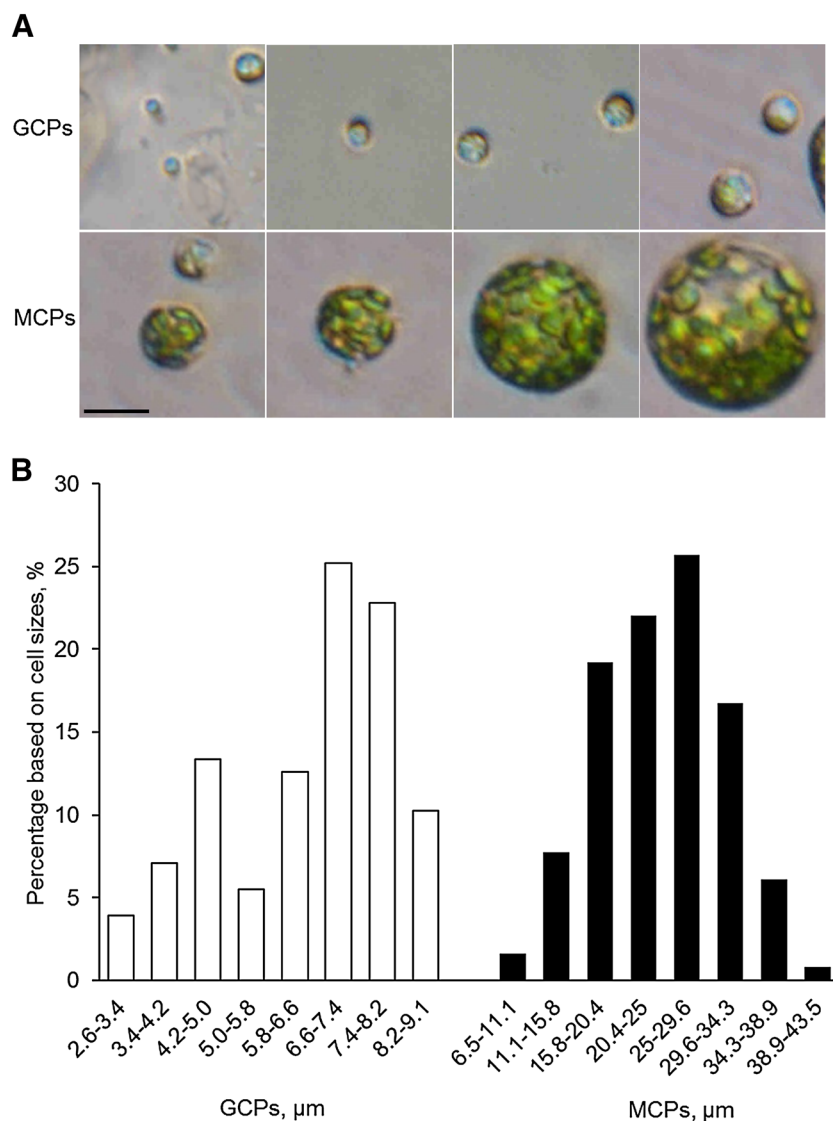
### Recovery rate of GCPs

The recovery rate (RR) of GCPs was calculated using the following formula:  $\text{RR} = (\text{GCP yield}) / (\text{total number of stomata} \times 2) \times 100\%$ . In this study, only abaxial epidermal peels of *ColLer* were used for GCP extraction, and GCP yield in this study was  $1.44 \times 10^6$  from 150  $\text{cm}^2$  of peels. *ColLer* had an average abaxial stomatal density 180 stomata per  $\text{mm}^2$ . Therefore, the total number of guard cells used in the extraction was  $1.44 \times 10^6 / (150 \times 100 \times 180 \times 2)$  resulting in a RR of 26.5%. The GCP yield in Pandey et al. (2002) was  $2.2 \times 10^6$  from 80 *Col-0* leaves. For the method of Pandey et al. (2002), mature leaf size was estimated at  $\pi \times 0.5 \times 1.5 = 2.355$   $\text{cm}^2$  assuming leaves are elliptical in shape and the stomatal density on the epidermal sides were 190 stomata per  $\text{mm}^2$  for the abaxial side and 150 stomata per  $\text{mm}^2$  for the adaxial side for *Col-0* (Lake and Wade 2009). Thus, the number of guard cells in Pandey et al. (2002) was  $2.2 \times 10^6 / [80 \times 2.355 \times 100 \times (190 + 150) \times 2]$ , which gives an RR of 17.2%.

### Discussion

To reveal the unique gene expression characteristics of different plant cell-types, single-cell-type transcriptomes have been examined in different plant species using

**Fig. 2** Distribution of diameters of guard cell protoplasts (GCPs) and mesophyll cell protoplasts (MCPs) of *Arabidopsis thaliana*. **a** Representative GCPs and MCPs showing differences in sizes. GCPs appear pale-green while MCPs appear dark-green. Scale bar represents 20  $\mu\text{m}$ . **b** Distribution of diameters of *Arabidopsis* GCPs and MCPs. Diameters of more than 200 protoplasts from three microscope views were measured



RNA-sequencing and microarray technologies. Transcriptomic studies of different cell-types usually share common biological functions and can be compared to reveal the conserved genes associated with a specific biological function (Leonhardt et al. 2004; Libault et al. 2010, 2017; Deal and Henikoff 2011; Liu et al. 2013). Unlike pollen and root hairs that can be isolated in large quantities without digestion of cell wall (Liu et al. 2013; He et al. 2015), guard cells are tightly connected to epidermal cells and require enzymatic methods to obtain GCPs (Pandey et al. 2002; Leonhardt et al. 2004). Our study has developed a promising protocol for producing suspensions of GCPs with a high yield and purity using relatively fast and mild extraction conditions.

Buffer solutions mimicking normal intracellular pH, ionic conditions and osmolality are used in many studies for maintaining stomatal activity for at least a few hours after peeling the epidermis from leaves (Chen et al. 2012; Wang et al. 2013; Jezek and Blatt 2017). Therefore, in the GCP protocol

reported here, it is likely that normal guard cell activities are maintained and minimal physical damage is caused on these epidermal peels in comparison to tissue blending methods that, essentially, break down all leaf tissues to obtain a suspension containing millions of dead, wound, and live cells including both GCPs and MCPs. Even for those live cells, there may have been a certain level of mechanical damage, potentially affecting the isolation and purification of GCPs and their quality for omics research. The recovery rate of GCPs after extraction and shorter extraction time suggests that the revised protocol causes less stress, thus improving the yield of GCPs. A recovery rate of 17% was calculated for the protocol of Pandey et al. (2002), which may suggest that many guard cells were damaged during the blending process.

An appropriate digestion time is critical for protoplast isolation, because a short digestion may not yield enough protoplasts while over digestion during extraction decreases GCP yields and leads to RNA degradation (Obulareddy et al.

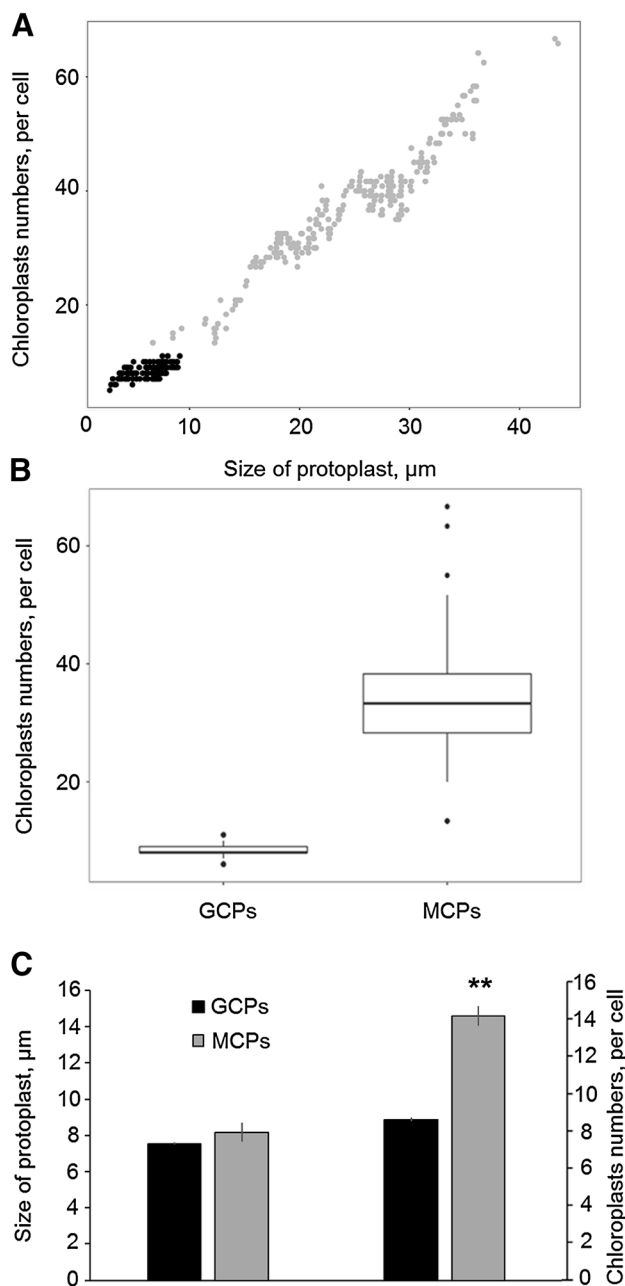


**Fig. 3** Estimated numbers of chloroplasts in guard cell protoplasts (GCPs) and mesophyll cell protoplasts (MCPs) of *Arabidopsis thaliana*. **a** Scatter plot showing the relationship between protoplast sizes (x axis) and chloroplast numbers (y axis). There is a correlation between protoplast sizes and chloroplast numbers in GCPs ( $y = 0.43x + 5.67$ ,  $R^2 = 0.32$ ,  $P < 0.01$ ) but a significant linear correlation ( $y = 1.69x + 2.71$ ,  $R^2 = 0.91$ ,  $P < 0.01$ ) was found in the MCPs data set. For the correlation analysis, a two-tailed Pearson test was used. **b** Box plot of chloroplasts numbers in GCPs and MCPs. Black dots represent outlying values. At least three microscope views, in a single plane, from two biological replicates were checked and more than 250 separated protoplasts were investigated in MCPs and GCPs. **c** Comparison of protoplast sizes and chloroplast numbers in GCPs and MCPs that overlap in size. Error bars are the standard errors of the means. Data were subjected to Student's *t* tests. \*\*Significant difference at  $P < 0.01$

2013). Epidermal peels contain a single layer of cells, and the cell walls can be digested from both sides. After incubation in ESI, epidermal cell walls are digested and epidermal cell protoplasts burst due to the low solution osmolality of ESI (Pandey et al. 2002); however, guard cells remain intact (Fig. 1b). During the second digestion in ESII, guard cell walls are further digested, and the increased solution osmolality leads to the release of guard cell protoplasts (Fig. 1c). Compared with the existing protocols (Kruse et al. 1989; Pandey et al. 2002; Yao et al. 2018), our protocol using detached epidermis requires 15% less digestion time. However, the use of microscopic observations during incubation in both ESI and ESII is recommended to secure an optimal digestion time (Fig. 1b, c).

Filtering procedures have been included in most GCPs extraction protocols (Kruse et al. 1989; Pandey et al. 2002; Yao et al. 2018) on the assumption that differences in protoplast sizes between GCPs and other leaf protoplasts are large enough allow separation by filtration. Measurement of the *Vicia faba* GCPs sizes showed that most of the GCPs were less than 20 μm in diameter (Kruse et al. 1989), leading to the choice of 20 μm nylon mesh as a final filtering process (Pandey et al. 2002). However, few studies have compared the sizes of protoplasts from different cell types. In our study, the diameters of GCPs were between 2.6 and 9.1 μm while the sizes of MCPs were between 6.5 and 43.5 μm (Fig. 2b). Therefore, there is an overlap in size between GCPs and MCPs, and 28.6% of MCPs were found to be less than 20 μm in diameter and 9.5% of MCPs were smaller than 15 μm (Fig. 2b). Given that protoplasts are highly flexible, a large number of MCPs can be expected to go through a 20 μm or 15 μm nylon mesh (Pandey et al. 2002; Yao et al. 2018). This suggests that contamination with MCPs during GCPs extraction using mechanical blending cannot be avoided by filtering alone. To overcome this problem, a smaller size mesh (10 μm) has been suggested for use. However, it is difficult to filter protoplast suspensions through such a small mesh due to surface tension, which will lead to a low protoplast yields. An alternative approach is to reduce the number of small mesophyll cells from the start of the extraction process. Our protocol minimises the numbers of mesophyll cells by employing detached epidermal peels and by removing visible, green patches of mesophyll cells that remain attached to the peels (Fig. 1). As a result, a GCP purity of more than 97% was obtained (Fig. 4a). There was less than 3% contamination with MCPs, which was perhaps due to the small number of mesophyll cells that may still remain attached to the epidermal peels.

In an earlier report, a higher purity of GCPs at 98–99.5% was reported without clarifying the process for calculating purity or the cause of contamination (Pandey et al. 2002). Due to the overlap in protoplast size, it is possible that an overestimation in GCP purity was obtained.

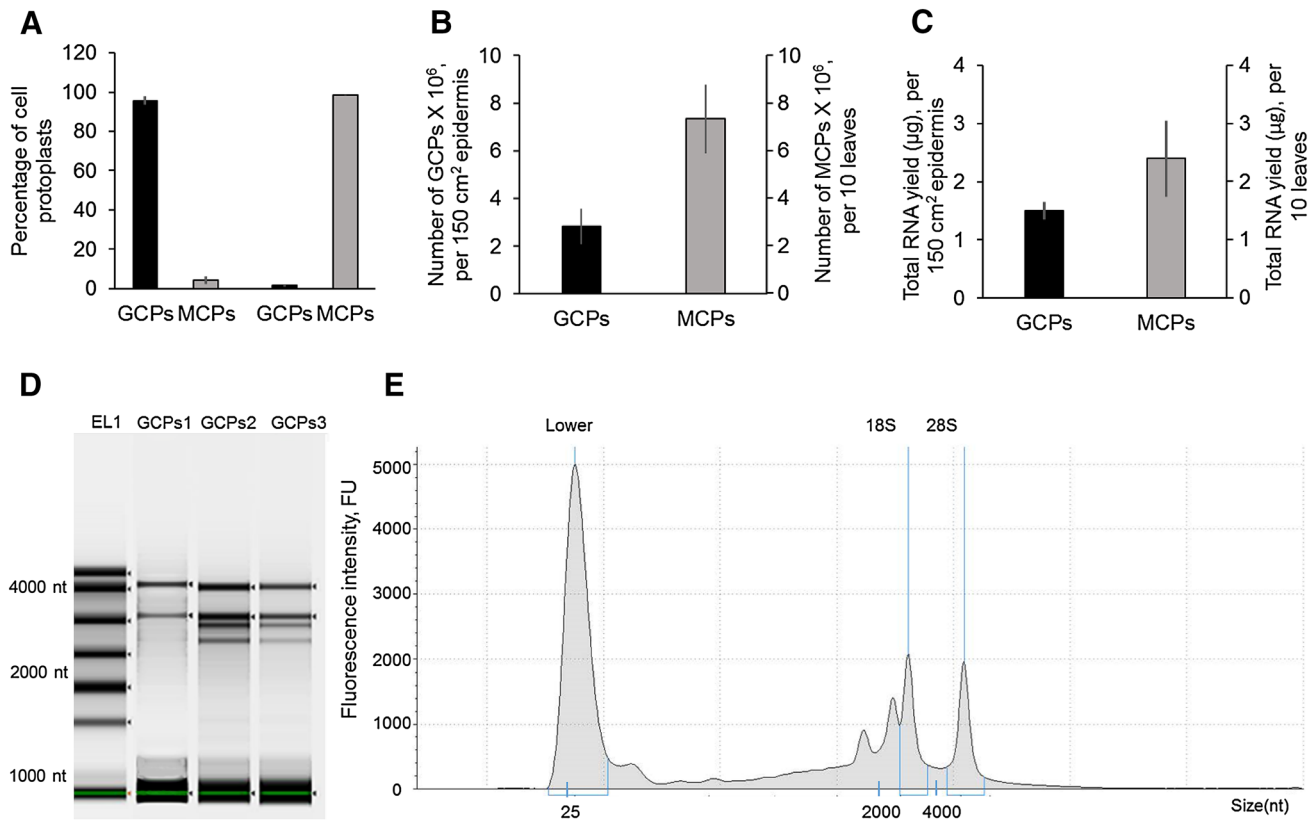


**Fig. 4** Purity, cell yield and total RNA yield from guard cell protoplasts (GCPs) and mesophyll cell protoplasts (MCPs) of *Arabidopsis thaliana*. **a** Bar graphs of purity of target protoplasts in GCPs and MCPs extractions. Values of GCPs extraction were calculated from three microscope views from two independent extractions  $\pm$  standard errors, and values of MCPs are from three independent extractions  $\pm$  standard errors. **b** GCP yield from approx. 150 cm<sup>2</sup> *Arabidopsis* abaxial epidermal peels and MCP yield from approx. 10 *Arabidopsis* leaves. The yield of GCPs was calculated from three microscope views from two independent extractions  $\pm$  standard errors and the yield of MCPs was calculated from three independent extractions

$\pm$  standard errors. **c** Comparison of total RNA yield extracted from GCPs (from approx. 150 cm<sup>2</sup> *Arabidopsis* abaxial epidermal peels) and RNA yield from MCPs (from approx. 10 leaves). Results are means from three biological replicates  $\pm$  standard errors. **d** Gel images from Agilent Bioanalyzer for analysing GCPs total RNA quality. Three replicates of GCPs were analysed and distinctive 18S and 28S ribosomal RNA bands were observed in all samples. **e** Densitometry of total RNA extracted from GCPs, showing clear peaks of the 18 s and 28 s ribosomal RNAs. *EL* electropherogram ladder, *nt* nucleotide

**Table 1** Quality control data from RNA extracts from guard cell protoplasts (GCPs) and mesophyll cell protoplasts (MCPs) of *Arabidopsis thaliana*

Sample	Raw base (Mbases)	Raw reads (Mbases)	Clean base (Mbases)	Clean reads (Mbases)	% of $\geq$ Q30 Bases	Read length	GC(%)
GCPs rep 1	2443.46	19.46	2195.53	17.72	89.95	126	48.03
GCPs rep 2	2037.61	16.23	1829.24	14.80	89.77	126	47.52
GCPs rep 3	2319.14	18.47	2076.05	16.77	89.52	126	48.49
MCPs rep 1	2850.61	22.80	2366.05	19.40	83.00	125	45.63
MCPs rep 2	2849.78	22.80	2357.71	19.32	82.73	125	45.49
MCPs rep 3	2820.29	22.56	2333.60	19.14	82.74	125	45.19

When determining purity, it is important to consider whether MCPs and GCPs in the overlapping size classes are distinguishable from each other. This study investigated chloroplast numbers in both MCPs and GCPs. In

general, MCPs have a higher number of chloroplasts than GCPs, and it seems that GCPs have tight genetic control of chloroplast numbers. The differences in chloroplast numbers may be due to the fact that in GCPs chloroplast are

**Table 2** Read mapping information derived from RNA extracts from guard cell protoplasts (GCPs) and mesophyll cell protoplasts (MCPs) of *Arabidopsis thaliana*

Sample	Total reads	Unmapped reads	Unique map	Non-unique map	Splice reads
GCPs rep 1	18,577,784	1,005,061 (5.41%)	13,035,179 (70.2%)	4,537,544 (24.42%)	3,459,440 (18.62%)
GCPs rep 2	15,521,374	514,296 (3.31%)	11,493,017 (74.0%)	3,514,061 (22.64%)	297,433 (19.16%)
GCPs rep 3	17,579,406	592,267 (3.37%)	11,899,845 (67.7%)	5,087,294 (28.94%)	2,911,096 (16.56%)
MCPs rep 1	20,338,278	865,484 (4.26%)	19,183,727 (94.3%)	289,067 (1.42%)	6,769,271 (33.28%)
MCPs rep 2	20,255,296	842,658 (4.16%)	19,106,891 (94.3%)	305,747 (1.51%)	6,150,641 (30.37%)
MCPs rep 3	20,066,022	752,709 (3.75%)	19,057,323 (95.0%)	255,990 (1.28%)	6,532,161 (32.55%)

not predominantly used for photosynthesis but for other purposes such as the generation of signals for stomatal closure (Lawson 2009). For GCPs and MCPs of overlapping sizes, chloroplast numbers in MCPs are also significantly ( $P < 0.001$ ) higher than those in GCPs (Fig. 3c). Thus, it is easy to distinguish MCPs from GCPs from each other based on their appearance, and this difference can be used in calculating protoplast purity.

Grass stomata have a complex structure (Cai et al. 2017; Raissig et al. 2017) consisting two guard cells and two subsidiary cells, which has enabled a fast stomatal response for grass species to adapt to the changing climate and to be some of dominant agricultural crops during their evolution and domestication (Chen et al. 2017; Wang et al. 2018). The current method of guard cell protoplast isolation is suitable for *Arabidopsis* or potentially for some of the eudicots. However, isolation of guard cell protoplasts from epidermal peels of other major clades of plants (Zhao et al. 2019), especially from the monocots will need significant refinement and modification of the current protocol. A major challenge will be the isolation and separation of grass guard cells from subsidiary cells and other cell types. Molecular probes and flow cytometry are likely to be employed along with this protocol to increase the purity of grass guard cell protoplasts, rendering future investigation.

In summary, this protocol provides evidence showing the high quality of RNA that can be extracted and transcribed from protoplasts from the two cell types using the procedures. These methods provide alternative choices for researchers to conduct cell-specific studies, particularly using guard cells, and can also be adapted to isolate tissue-specific protoplast from other plant species. The higher purity of GCPs and reduced stress imposed on the protoplasts during isolation may facilitate more accurate single-cell-type omics studies. Future studies could also compare the transcriptome or micro-RNAs of *Arabidopsis* GCPs prepared using the various methods of protoplast isolation to determine differences in gene expression. In addition, the use of flow cytometry could be explored to remove MCPs, especially if the purity of GCPs is lower than 90%.

## Materials and methods

### Plant growth

Seeds of the *Arabidopsis thaliana* wild-type, Col $Ler$  (a cross of Columbia and Landsberg erecta ecotypes), were sterilized with 10% bleach (White King, Pental Limited, Victoria, Australia) then washed thoroughly with autoclaved Milli-Q (Millipore Milli-Q® Integral 10, MERCK, Australia) water. Subsequently, the seeds were germinated in autoclaved potting mix (compost:perlite:vermiculite = 3:1:1 by volume) and kept at 4 °C for three days. The resulting seedlings were grown under  $120 \pm 20 \mu\text{mol}$  of photons  $\text{m}^{-2} \text{s}^{-1}$ , a 16 h photoperiod, a temperature of 22–25 °C, and 70% humidity in a growth chamber (Thermoline Scientific, Whetherill Park, NSW, Australia). Nutrients were supplemented to the plants as half strength Hoagland solution (Hoagland and Arnon 1950) once in the first 2 weeks and twice in the 3rd and 4th weeks.

### Isolation of GCPs from *Arabidopsis thaliana*

The protocol for GCPs isolation was modified from Kruse et al. (1989) and Pandey et al. (2002). Instead of blending whole leaves, we detached ~200 abaxial epidermal peels from 100 healthy, mature leaves. Young (not fully expanded) and old leaves were not used because of the difficulty in obtaining sufficient areas of epidermal peels and low GCP yields, respectively. A three step procedure was used for peeling the leaves avoiding the major veins. A pair of forceps with fine tips was used to pierce the leaf and to form a small (5 × 3 mm) convex opening. Then, the forceps were used to gently peel the epidermis to produce a long strip. Any visible green parts of the peeled epidermal strips were cut off before immersing them into cold Opening Buffer (OB, 50 mM KCl, 5 mM MES, 50  $\mu\text{M}$  CaCl<sub>2</sub>, 0.1% PVP-40, pH 6.1 adjusted with KOH) with the inner side of epidermal peels facing the solution to avoid guard cell dehydration.

Three digestion solutions were then used for GCP extraction: (1) Basic Solution (BS): 5 mM MES, 0.5 mM CaCl<sub>2</sub>, 0.5 mM MgCl<sub>2</sub>, 10  $\mu\text{M}$  KH<sub>2</sub>PO<sub>4</sub>, 0.5 mM ascorbic acid, and

0.55 M sorbitol (pH adjusted to 5.5 with HCl, 515 mOsm); (2) Enzyme Solution I (ESI): 0.7% (w/v) cellulysin, 0.1% (w/v) polyvinyl pyrrolidone 4000 (PVP-40), 0.25% (w/v) bovine serum albumin (BSA), 0.5 mM L-ascorbic acid prepared in 55% BS and 45% (v/v) Milli-Q water, 320 mOsm; and (3) Enzyme Solution II (ESII): 1.3% (w/v) Onozuka RS cellulose, 0.0075% (w/v) pectolyase Y-23, 0.25% BSA, 0.5 mM L-ascorbic acid (prepared in BS, 600 mOsm). The pH of ESII was reduced to 3.5 with HCl to inactivate contaminating proteases existing in commercial cell wall digestion enzymes. The pH was then adjusted back to 5.5 with KOH before filtering through 0.22 µm filters (SFCA, Thermofisher Scientific, USA) to purify the solution.

The peels were then dip-rinsed with cold Milli-Q water to wash off the OB buffer and then transferred into a 50 mL flask and immersed in 10 mL ESI. The flask was then kept dark in a temperature-controlled shaker (Ratek Instruments Pty Ltd, Victoria, Australia) at 28 °C and 90 rpm for 20 min. After this time and at subsequent 5 min intervals, the peels were examined using a microscope to check their digestion status. Compared with pre-digested epidermal peels (Fig. 1a), ideal digestion in ESI results in more transparent peels with thinner guard cell walls and the disappearance of epidermal cell walls (Fig. 1b). This was usually achieved after a total of 25 min in ESI, and all the guard cells were intact after the digestion (Fig. 1).

In order to reduce sudden changes in osmolality that may damage guard cells, 30 mL of BS was added to the suspension and the suspension gently shaken for 5 min at 90 rpm. The digested peels were then collected by filtering the suspension through a 200 µm nylon mesh (Thomas Scientific, USA) and then transferred to a 50 mL flask containing 10 mL of ESII. The flask containing ESII and peels was incubated at 20 °C and 40 rpm in the dark for 40 min. After 40 min digestion in ESII and then at subsequent 5 min intervals, checks were conducted until most of the guard cell protoplasts were released from the peels (Fig. 1c); this typically occurred after 10 min in ESII. After sufficient digestion, the flask was gently shaken by hand to release remaining GCPs from the epidermal peels until few guard cells were visible on the epidermal peels under the microscope (Fig. 1d). Then, the mixture was filtered through a 20 µm nylon mesh, and the residue on the mesh gently rinsed by 30 mL BS. The filtrate was placed in 50 mL Falcon tubes (Sigma-Aldrich, NSW, Australia) and centrifuged for 5 min at 200×g at 4 °C. The supernatant was carefully removed after which 10 mL aliquots of the remaining filtrate were transferred into 15 mL Falcon tubes (Sigma-Aldrich, NSW, Australia) and centrifuged for another 5 min at 200×g at 4 °C. The pellets were then resuspended in 1 mL of BS. Usually, during the second centrifuging process, the suspension is largely composed of GCPs but is contaminated with a small number of MCPs and chloroplasts. To further purify

the GCPs, 500 µL Histopaque (No. 1077, Sigma, Castle Hill, Australia) was placed into each of two 1.5 mL Eppendorf tubes. Then, 500 µL of GCP suspension was carefully transferred on top of the Histopaque and centrifuged at 200×g for 15 min at 4 °C. After centrifuging, an opaque layer of GCPs was concentrated at the interfaces of the two solutions. These layers were carefully collected using a pipette and the volume adjusted to 1 mL with BS before centrifuging for 5 min at 200×g at 4 °C. The supernatants were carefully removed, and the pellets were slowly resuspended with 500 µL BS. The GCPs were incubated on ice for 1 h in the dark to allow the recovery of the protoplast membranes (Pandey et al. 2002). The quality of GCPs suspension was checked using a microscope (Fig. 1e, h).

### Isolation of MCPs from *Arabidopsis thaliana*

The protocol for MCP extraction was modified from Bonales-Alatorre et al. (2013). Four solutions were used for MCP isolation: (1) Wash Solution (WS): 10 mM KCl, 10 mM CaCl<sub>2</sub>, 2 mM MES, 20 mM glucose and 20 mM sucrose (the osmolality was adjusted to 750–800 mOsm with sorbitol and the pH to 5.7 with KOH); (2) Release Solution (RS): 10 mM KCl, 2 mM MgCl<sub>2</sub>, 2 mM MES (the osmolality was adjusted to 380 mOsm with sorbitol and the pH to 5.7 with KOH); (3) Maintaining Solution (MS): 2 mM CaCl<sub>2</sub>, 5 mM KCl, 2 mM MES (the osmolality adjusted between 500 and 570 mOsm with sorbitol and the pH to 7.4 with KOH); and (4) Enzyme Solution (ES): 2% (w/v) cellulase (Onozuka RS, Yakult Pharmaceutical, Tokyo, Japan), 1.2% (w/v) cellulysin (Calbiochem, San Diego, USA), 0.1% (w/v) pectolyase Y-23 (Kyowa Chemical Industry, Sakaide, Japan) and 0.1% (w/v) BSA (Sigma-Aldrich, USA), prepared with wash solution (osmolality was adjusted to 750–800 mOsm with sorbitol).

To obtain MCPs, the abaxial epidermis was peeled from ten leaves and then the remaining leaf segments were cut into 3 mm × 10 mm pieces avoiding the main veins. The leaf segments were placed in 1.5 mL of ES in a glass-bottomed Petri dish (MatTek corporation, 200 Homer Avenue Ashland, MA 31721, USA) with the exposed mesophyll cells facing the solution. The Petri dishes were kept in the dark and incubated for 40 min at 28 °C in a rotary shaker at 90 rpm. After 30 min incubation, it is important to check that the leaf segments are neither hard nor plasmolysed to ensure a high yield and quality of MCPs. The leaf tissue can then be incubated for a further 10 min. Digested leaf segments were picked up using forceps and gently washed in WS and subsequently incubated in RS at 25 °C for 10 min during which time the solution turns pale green. Leaf segment residues were then separated by gently spinning the Petri dish; this concentrates the MCPs at the centre of the Petri dish due to the centripetal force. Excess liquid was carefully removed



using a pipette avoiding the areas with MCPs. The suspension was then transferred to a 1.5 mL Eppendorf tube and centrifuged for 5 min at 300×g. Finally, the pellets were resuspended in 500 µL MS and were incubated on ice in the dark for 1 h for the MCPs to recover (Fig. 1f, g).

### Size and chloroplast distribution in GCPs and MCPs

Images were taken using a microscope with a NIS-F1 CCD camera and a DS-U3 controller (Nikon, Tokyo, Japan), and were processed and analysed using ImageJ software (NIH, USA). GCPs and MCPs from three biological replicates were analysed to determine their diameters and chloroplast numbers. Diameters data of protoplasts (both GCPs and MCPs) were analysed by SPSS (IBM SPSS statistics 25, USA) using a One-Sample Kolmogorov–Smirnov Test non-parametric test for normality. Sizes of GCPs and MCPs were separated into eight groups by introducing a 0.8 µm interval and a 4.6 µm interval, respectively. To estimate chloroplast numbers in protoplasts, chloroplasts were manually counted in a single plane of view using ImageJ. Box plots of chloroplast numbers were generated using R Studio (v1.1.1456) and the ggplot2 package (Wickham and Chang 2008).

### Protoplast yield and RNA quality

Protoplast yields were estimated from representative images taken using an inverted microscope. The purity of GCPs and MCPs and estimated protoplasts yields were calculated based on counts in ImageJ. GCPs from MCPs were identified on the basis of their sizes, chloroplast numbers and colour. For similar sized MCPs and GCPs, MCPs were in dark green due to their large number of chloroplasts. This was considered when calculating protoplast purity. At least three microscopic fields of three separate protoplast isolations from different days were examined. For RNA extraction, protoplasts were centrifuged for 5 min at 200×g. After removing excess liquid, samples were snap-frozen with liquid nitrogen. RNA was extracted using an RNeasy Plant Mini Kit (Qiagen, CA, USA). RNA quality was determined using an Agilent Bioanalyzer 2100 and an Agilent RNA 600 Pico Kit at the NGS Facility, Western Sydney University, Australia.

**Acknowledgements** This work was supported by Australian Research Council (ARC) (Grant No. DE1401011143) and Horticulture Innovation Australia (HIA) projects (LP18000, VG16070, VG17003) to Z.H.C. We thank Ms Linda Westmoreland, Dr Sumedha Dharmaratne and Ms. Sharleen Hamersma for their technical assistance.

**Author contributions** ZHC conceived and directed the study; CZ and DR conducted the experiments; CZ, ZHC, AMH, and PH wrote the manuscript; All authors read and approved the final manuscript.

### Compliance with ethical standards

**Conflict of interest** The authors declare that they have no competing interests.

### References

- Allen GJ, Sanders D (1994) Two voltage-gated, calcium release channels coreside in the vacuolar membrane of broad bean guard cells. *Plant Cell* 6:685–694
- Allen GJ, Kuchitsu K, Chu SP, Murata Y, Schroeder JI (1999) *Arabidopsis* *abi1-1* and *abi2-1* phosphatase mutations reduce abscisic acid-induced cytoplasmic calcium rises in guard cells. *Plant Cell* 11:1785–1798
- Aubry S, Aresheva O, Reyna-Llorens I, Smith-Unna R, Hibberd JM, Genty B (2016) A specific transcriptome signature for guard cells from the C4 plant *Gynandropsis gynandra*. *Plant Physiol* 170:1345–1357
- Bonales-Alatorre E, Shabala S, Chen Z-H, Pottosin I (2013) Reduced tonoplast fast-activating and slow-activating channel activity is essential for conferring salinity tolerance in a facultative halophyte, quinoa. *Plant Physiol* 162:940–952
- Brennecke P et al (2013) Accounting for technical noise in single-cell RNA-seq experiments. *Nat Methods* 10:1093–1095
- Cai S, Papanatsiou M, Blatt MR, Chen ZH (2017) Speedy grass stomata: emerging molecular and evolutionary features. *Mol Plant* 10:912–914
- Chen ZH, Hills A, Lim CK, Blatt MR (2010) Dynamic regulation of guard cell anion channels by cytosolic free Ca<sup>2+</sup> concentration and protein phosphorylation. *Plant J* 61:816–825
- Chen ZH, Eisenach C, Xu XQ, Hills A, Blatt MR (2012) Protocol: optimised electrophysiological analysis of intact guard cells from *Arabidopsis*. *Plant Methods* 8:1–15
- Chen ZH et al (2016) Nitrate reductase mutation alters potassium nutrition as well as nitric oxide-mediated control of guard cell ion channels in *Arabidopsis*. *New Phytol* 209:1456–1469
- Chen ZH et al (2017) Molecular evolution of grass stomata. *Trends Plant Sci* 22:124–139
- Chen G et al (2019) Leaf epidermis transcriptome reveals drought-induced hormonal signaling for stomatal regulation in wild barley. *Plant Growth Regul* 87:39–54
- Chung HS, Koo AJ, Gao X, Jayanty S, Thines B, Jones AD, Howe GA (2008) Regulation and function of *Arabidopsis* JASMONATE ZIM-domain genes in response to wounding and herbivory. *Plant Physiol* 146:952–964
- Deal RB, Henikoff S (2011) The INTACT method for cell type-specific gene expression and chromatin profiling in *Arabidopsis thaliana*. *Nat Protoc* 6:56–68
- Fairley-Grenot K, Assmann S (1992) Whole-cell K<sup>+</sup> current across the plasma membrane of guard cells from a grass: *Zea mays*. *Planta* 186:282–293
- Fitzsimons PJ, Weyers JD (1983) Separation and purification of protoplast types from *Commelina communis* L. leaf epidermis. *J Exp Bot* 34:55–66
- Franks PJ, Doheny-Adams TW, Britton-Harper ZJ, Gray JE (2015) Increasing water-use efficiency directly through genetic manipulation of stomatal density. *New Phytol* 207:188–195
- Gudesblat GE, Torres PS, Vojno AA (2009) Stomata and pathogens: warfare at the gates. *Plant Signal Behav* 4:1114–1116
- Guo FQ (2002) The nitrate transporter AtNRT1.1 (CHL1) functions in stomatal opening and contributes to drought Susceptibility in *Arabidopsis*. *Plant Cell* 15:107–117

- Hall RD et al (1996) A high efficiency technique for the generation of transgenic sugar beets from stomatal guard cells. *Nat Biotechnol* 14:1133
- Hara K, Yagi M, Koizumi N, Kusano T, Sano H (2000) Screening of wound-responsive genes identifies an immediate-early expressed gene encoding a highly charged protein in mechanically wounded tobacco plants. *Plant Cell Physiol* 41:684–691
- He X, Zeng J, Cao F, Ahmed IM, Zhang G, Vincze E, Wu F (2015) *HvEXPB7*, a novel  $\beta$ -expansin gene revealed by the root hair transcriptome of Tibetan wild barley, improves root hair growth under drought stress. *J Exp Bot* 66:7405–7419
- Hedrich R, Shabala S (2018) Stomata in a saline world. *Curr Opin Plant Biol* 46:87–95
- Hedrich R, Busch H, Raschke K (1990)  $\text{Ca}^{2+}$  and nucleotide dependent regulation of voltage dependent anion channels in the plasma membrane of guard cells. *EMBO J* 9:3889–3892
- Henriksen GH, Assmann SM (1997) Laser-assisted patch clamping: a methodology. *Pflügers Arch* 433:832–841
- Hetzl J, Duttke SH, Benner C, Chory J (2016) Nascent RNA sequencing reveals distinct features in plant transcription. *Proc Natl Acad Sci USA* 113:12316–12321
- Hoagland DR, Arnon DI (1950) The water-culture method for growing plants without soil. Circular California Agricultural Experiment Station, Berkeley, p C347
- Hughes J et al (2017) Reducing stomatal density in barley improves drought tolerance without impacting on yield. *Plant Physiol* 174:776–787
- Jezeq M, Blatt MR (2017) The membrane transport system of the guard cell and its integration for stomatal dynamics. *Plant Physiol* 174:487–519
- Jin X, Wang RS, Zhu M, Jeon BW, Albert R, Chen S, Assmann SM (2013) Abscisic acid-responsive guard cell metabolomes of *Arabidopsis* wild-type and *gpa1* G-protein mutants. *Plant Cell* 25:4789–4811
- Kruse T, Tallman G, Zeiger E (1989) Isolation of guard cell protoplasts from mechanically prepared epidermis of *Vicia faba* leaves. *Plant Physiol* 90:1382–1386
- Lahav M, Abu-Abied M, Belausov E, Schwartz A, Sadot E (2004) Microtubules of guard cells are light sensitive. *Plant Cell Physiol* 45:573–582
- Lake JA, Wade RN (2009) Plant-pathogen interactions and elevated  $\text{CO}_2$ : morphological changes in favour of pathogens. *J Exp Bot* 60:3123–3131
- Lawson T (2009) Guard cell photosynthesis and stomatal function. *New Phytol* 181:13–34
- Leonhardt N, Kwak JM, Robert N, Waner D, Leonhardt G, Schroeder JI (2004) Microarray expression analyses of *Arabidopsis* guard cells and isolation of a recessive abscisic acid hypersensitive protein phosphatase 2C mutant. *Plant Cell* 16:596–615
- Libault M et al (2010) Complete transcriptome of the soybean root hair cell, a single-cell model, and its alteration in response to *Bradyrhizobium japonicum* infection. *Plant Physiol* 152:541–552
- Libault M, Pingault L, Zogli P, Schiefelbein J (2017) Plant systems biology at the single-cell level. *Trends Plant Sci* 22:949–960
- Lind C et al (2015) Stomatal guard cells co-opted an ancient ABA-dependent desiccation survival system to regulate stomatal closure. *Curr Biol* 25:928–935
- Liu Y et al (2013) Functional conservation of MIKC\*-type MADS box genes in *Arabidopsis* and rice pollen maturation. *Plant Cell* 25:1288–1303
- Mäser P, Leonhardt N, Schroeder JI (2003) The clickable guard cell: electronically linked model of guard cell signal transduction pathways. *The Arabidopsis Book*, New York
- Melotto M, Underwood W, Koczan J, Nomura K, He SY (2006) Plant stomata function in innate immunity against bacterial invasion. *Cell* 126:969–980
- Meyer S et al (2010) AtALMT12 represents an R-type anion channel required for stomatal movement in *Arabidopsis* guard cells. *Plant J* 63:1054–1062
- Misra BB, Acharya BR, Granot D, Assmann SM, Chen S (2015) The guard cell metabolome: functions in stomatal movement and global food security. *Front Plant Sci* 6:334
- Obulareddy N, Panchal S, Melotto M (2013) Guard cell purification and RNA isolation suitable for high-throughput transcriptional analysis of cell-type responses to biotic stresses. *Mol Plant Microbe Interact* 26:844–849
- Palevitz B (1981) The structure and development of stomatal cells. *Stomatal Physiol* 8:1–23
- Pandey S, Wang XQ, Coursol SA, Assmann SM (2002) Preparation and applications of *Arabidopsis thaliana* guard cell protoplasts. *New Phytol* 153:517–526
- Petropoulos S et al (2016) Single-cell RNA-seq reveals lineage and X chromosome dynamics in human preimplantation embryos. *Cell* 165:1012–1026
- Quintana E, Shackleton M, Sabel MS, Fullen DR, Johnson TM, Morrison SJ (2008) Efficient tumour formation by single human melanoma cells. *Nature* 456:593–598
- Raissig MT, Matos JL, Gil MX, Kornfeld A, Bettadapur A, Abrash E, Allison HR, Badgley G, Vogel JP, Berry JA, Bergmann DC (2017) Mobile MUTE specifies subsidiary cells to build physiologically improved grass stomata. *Science* 355:1215–1218
- Reymond P, Weber H, Damond M, Farmer EE (2000) Differential gene expression in response to mechanical wounding and insect feeding in *Arabidopsis*. *Plant Cell* 12:707–719
- Robaina-Estévez S, Daloso DM, Zhang Y, Fernie AR, Nikoloski Z (2017) Resolving the central metabolism of *Arabidopsis* guard cells. *Sci Rep* 7:8307
- Schnabl H, Bornman CH, Ziegler H (1978) Studies on isolated starch-containing (*Vicia faba*) and starch-deficient (*Allium cepa*) guard cell protoplasts. *Planta* 143:33–39
- Vahisalu T et al (2008) SLAC1 is required for plant guard cell S-type anion channel function in stomatal signalling. *Nature* 452:487–491
- Wang Y, Blatt MR (2011) Anion channel sensitivity to cytosolic organic acids implicates a central role for oxaloacetate in integrating ion flux with metabolism in stomatal guard cells. *Biochem J* 439:161–170
- Wang Y, Papanatsiou M, Eisenach C, Karnik R, Williams M, Hills A, Lew VL, Blatt MR (2012) Systems dynamic modeling of a guard cell  $\text{Cl}^-$  channel mutant uncovers an emergent homeostatic network regulating stomatal transpiration. *Plant Physiol* 160:1956–1967
- Wang Y, Chen ZH, Zhang B, Hills A, Blatt MR (2013) PYR/PYL/RCAR abscisic acid receptors regulate  $\text{K}^+$  and  $\text{Cl}^-$  channels through reactive oxygen species-mediated activation of  $\text{Ca}^{2+}$  channels at the plasma membrane of intact *Arabidopsis* guard cells. *Plant Physiol* 163:566–577
- Wang H, Lan P, Shen RF (2016) Integration of transcriptomic and proteomic analysis towards understanding the systems biology of root hairs. *Proteomics* 16:877–893
- Wang X, Chen ZH, Yang C, Zhang X, Jin G, Chen G, Wang Y, Holford P, Nevo E, Zhang G, Dai F (2018) Genomic adaptation to drought in wild barley is driven by edaphic natural selection at the Tabigha Evolution Slope. *PNAS* 115(20):5223–5228
- Ward JM, Schroeder JI (1994) Calcium-activated  $\text{K}^+$  channels and calcium-induced calcium release by slow vacuolar ion channels in guard cell vacuoles implicated in the control of stomatal closure. *Plant Cell* 6:669–683
- Wickham H, Chang W (2008) ggplot2: AN implementation of the Grammar of Graphics R package version 07. <https://cran.r-project.org/web/packages/ggplot2/index.html>

- Wu AR et al (2013) Quantitative assessment of single-cell RNA-sequencing methods. *Nat Methods* 11:41–46
- Yang Y, Costa A, Leonhardt N, Siegel RS, Schroeder JI (2008) Isolation of a strong *Arabidopsis* guard cell promoter and its potential as a research tool. *Plant Methods* 4:6
- Yang DL et al (2017) Calcium pumps and interacting BON1 protein modulate calcium signature, stomatal closure, and plant immunity. *Plant Physiol* 175:424–437
- Yao X, Zhao W, Yang R, Wang J, Zhao F, Wang S (2018) Preparation and applications of guard cell protoplasts from the leaf epidermis of *Solanum lycopersicum*. *Plant Methods* 14:26
- Zeiger E (1981) Novel approaches to the biology of stomatal guard cells: protoplast and fluorescence studies. *Stomatal Physiol SEB Semin Ser* 8:103–117
- Zeiger E, Hepler PK (1976) Production of guard cell protoplasts from onion and tobacco. *Plant Physiol* 58:492–498
- Zeng W, Melotto M, He SY (2010) Plant stomata: a checkpoint of host immunity and pathogen virulence. *Curr Opin Biotechnol* 21:599–603
- Zhao L, Sack FD (1999) Ultrastructure of stomatal development in *Arabidopsis* (*Brassicaceae*) leaves. *Am J Bot* 86:929–939
- Zhao C, Haigh AM, Holford P, Chen ZH (2018) Roles of chloroplast retrograde signals and ion transport in plant drought tolerance. *Int J Mol Sci* 19:963
- Zhao C, Wang Y, Chan KX et al (2019) Evolution of chloroplast retrograde signaling facilitates green plant adaptation to land. *PNAS* 116:5015–5020
- Zhu JK (2016) Abiotic stress signalling and responses in plants. *Cell* 167:313–324

**Publisher's Note** Springer Nature remains neutral with regard to jurisdictional claims in published maps and institutional affiliations.